

^{57}Fe Mossbauer effect in the compound $\text{Er}_2\text{Fe}_{17}\text{C}_{2.5}$ prepared by melt spinning

This article has been downloaded from IOPscience. Please scroll down to see the full text article.

1993 J. Phys.: Condens. Matter 5 2415

(<http://iopscience.iop.org/0953-8984/5/15/012>)

View [the table of contents for this issue](#), or go to the [journal homepage](#) for more

Download details:

IP Address: 171.66.16.96

The article was downloaded on 11/05/2010 at 01:16

Please note that [terms and conditions apply](#).

^{57}Fe Mössbauer effect in the compound $\text{Er}_2\text{Fe}_{17}\text{C}_{2.5}$ prepared by melt spinning

Lin-shu Kong†, Bao-gen Shen†, Lei Cao†, Hua-yang Gong‡ and Yi-long Chen‡

† State Key Laboratory of Magnetism, Institute of Physics, Chinese Academy of Sciences, Beijing 100080, People's Republic of China

‡ Department of Physics, Wuhan University, 430072 Wuhan, People's Republic of China

Received 20 October 1992, in final form 21 December 1992

Abstract. The compound $\text{Er}_2\text{Fe}_{17}\text{C}_{2.5}$ formed by melt spinning has the rhombohedral $\text{Th}_2\text{Zn}_{17}$ -type structure. The spin reorientation transition occurs at about 136 K. The ^{57}Fe Mössbauer effect was measured in the temperature range 12–300 K. From the acceptable fit we find that the effective hyperfine fields of various sites decrease in the order $6c > 18f > 18h > 9d$. The anisotropy of the effective hyperfine field is observed to be different for different sites. The temperature dependence of the quadrupole splitting shows a large increase at around T_{sr} with increasing temperature.

1. Introduction

The binary R_2Fe_{17} compounds, except for $\text{Tm}_2\text{Fe}_{17}$ at low temperatures, do not have an easy c axis because the crystal-field-induced anisotropy of the R sublattice is too weak to counterbalance the easy-plane anisotropy of the iron sublattice [1]. The ^{57}Fe Mössbauer spectra of these compounds have to be analysed with at least seven independent subspectra because of the effects of the dipole fields and the electric field gradients (EFGs) [2]. Such complex situations make it difficult to assign the components of the spectra to the iron sites. For this reason the results on the order of the hyperfine fields of early investigations are inconsistent [3–5].

Recently, it was found that nitrogen and carbon atoms can be introduced into the interstitial sites of the 2:17 ($\text{Th}_2\text{Zn}_{17}$ or $\text{Th}_2\text{Ni}_{17}$) compounds [6–10]. These interstitial atoms lead to an enhancement of the rare-earth sublattice anisotropy and give some 2:17 compounds an easy uniaxial anisotropy. This offers the possibility of distinguishing the subspectra corresponding to the iron sites because the 2:17 compounds with an easy magnetization direction parallel to the c axis can be analysed with only four subspectra.

In this work, we carried out ^{57}Fe Mössbauer experiments on the $\text{Er}_2\text{Fe}_{17}\text{C}_{2.5}$ compounds prepared by melt spinning and investigated the magnetic properties of the iron sublattice on a local scale.

2. Experiment

The $\text{Er}_2\text{Fe}_{17}\text{C}_{2.5}$ sample was prepared by arc melting appropriate amounts of Er, Fe–C alloys and Fe in a high-purity argon atmosphere. For homogenization the sample was

melted several times. After melting, the ingots were melt spun in a high-purity argon atmosphere using a copper quench wheel rotating at a surface velocity V_s of 10–20 m s⁻¹. The ribbons were about 1 mm wide and 20–30 μm thick. X-ray diffraction experiments were carried out to determine the crystallographic structure. In addition to the x-ray patterns, thermomagnetic analysis was used to identify the single phase. The spin reorientation was observed from the magnetization versus temperature curve measured at a low magnetic field with a vibrating-sample magnetometer. The ⁵⁷Fe Mössbauer spectra were recorded using a constant-acceleration spectrometer (Oxford MS-500) in transmission geometry with a ⁵⁷Co source which was kept at room temperature. Temperature control to better than ± 0.1 K was achieved by the use of a proportional temperature controller. The data were analysed using the program MOSFUN.

3. Experimental results and analysis

X-ray diffraction and thermomagnetic analysis show that the as-quenched sample $\text{Er}_2\text{Fe}_{17}\text{C}_{2.5}$ is almost single phase with very small amounts of $\alpha\text{-Fe}$. The sample crystallizes in the rhombohedral $\text{Th}_2\text{Zn}_{17}$ -type structure, different from that of the $\text{Er}_2\text{Fe}_{17}\text{C}_x$ compound prepared by a gas–solid reaction, which has the same hexagonal $\text{Th}_2\text{Ni}_{17}$ -type structure as its parent compound $\text{Er}_2\text{Fe}_{17}$ [11, 12]. The difference between the two 2:17 structures results from the different orders of the dumbbells of Fe atoms. There are four crystallographically non-equivalent Fe sites, denoted by the Wyckoff notation 6c, 9d, 18h and 18f (4f, 6g, 12k and 12j), in the $\text{Th}_2\text{Zn}_{17}$ ($\text{Th}_2\text{Ni}_{17}$) structure type.

A change in the easy-magnetization direction with increasing temperature is observed in $\text{Er}_2\text{Fe}_{17}\text{C}_{2.5}$ (figure 1). The spin reorientation temperature T_{sr} is 136 K, about 55 K higher than that of $\text{Er}_2\text{Fe}_{17}\text{C}$ [13]. This indicates that the Er sublattice anisotropy is enhanced by the interstitial C atoms. It followed that the easy-magnetization direction of $\text{Er}_2\text{Fe}_{17}\text{C}_{2.5}$, like that of $\text{Er}_2\text{Fe}_{17}\text{C}$, is parallel to the c axis below T_{sr} .

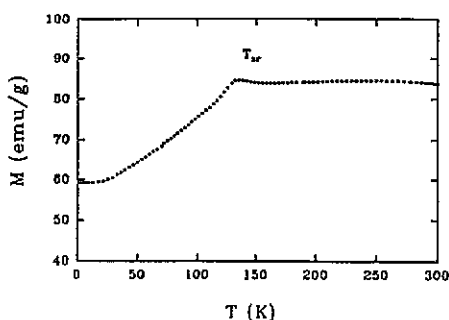


Figure 1. Thermomagnetic curve of as-quenched $\text{Er}_2\text{Fe}_{17}\text{C}_{2.5}$ in a field of 1 kOe.

The ⁵⁷Fe Mössbauer spectra of $\text{Er}_2\text{Fe}_{17}\text{C}_{2.5}$ in the temperature range 12–300 K are shown by the full circles in figure 2. When the easy-magnetization direction is parallel to the c axis, the spectra can be resolved into four Lorentzian sextets corresponding to the four crystallographically non-equivalent Fe sites, denoted by the Wyckoff notation 6c, 9d, 18h and 18f. When the easy-magnetization direction is perpendicular to the c axis, the spectra consist of more independent subspectra. Because of the differences in the angle

between the magnetization direction and the direction of the main axis of the electric field gradient tensor, the crystallographically equivalent iron atoms of a given subgroup will become magnetically non-equivalent. In addition, the magnetic dipolar fields also make the situation complicated. According to the calculation of the field gradients by means of a point charge model and the magnetic dipole field [2], the 2:17 compounds with the magnetization direction perpendicular to the c axis should be analysed with at least seven independent subspectra.

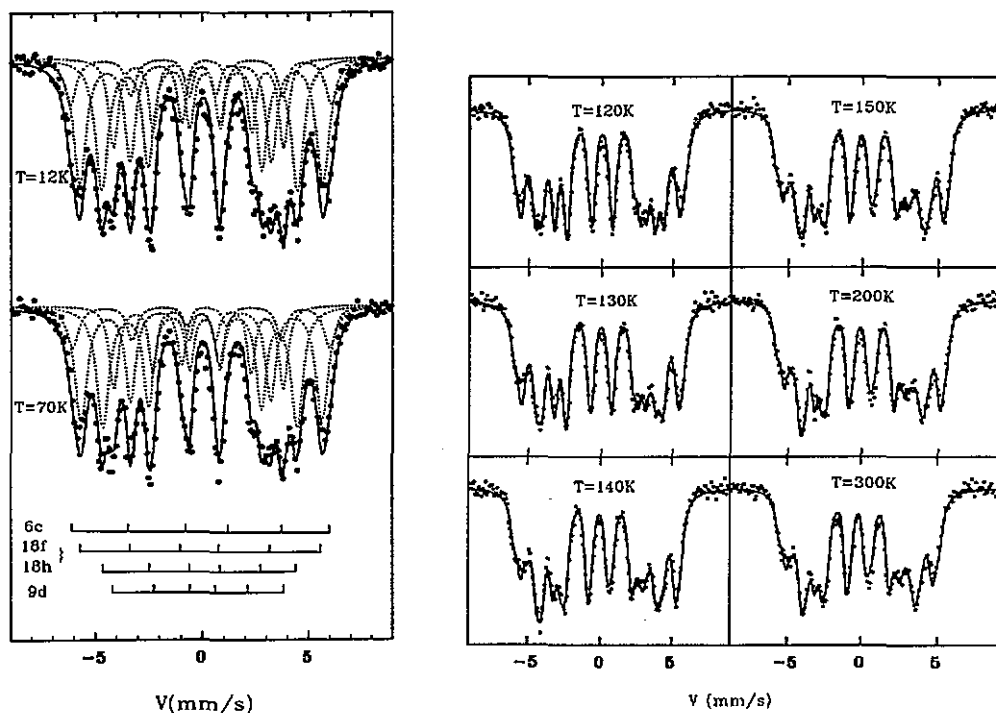


Figure 2. ^{57}Fe Mössbauer spectra of $\text{Er}_2\text{Fe}_{17}\text{C}_{2.5}$ at various temperatures with the fits shown as full curves. The decomposition of the spectra into subspectra corresponding to the four non-equivalent iron sites is indicated below the spectra on the left-hand side.

In order to give a safer conclusion in the fits, we first analysed the spectra of $\text{Er}_2\text{Fe}_{17}\text{C}_{2.5}$ below T_{sr} . Least-squares fits were carried out on a sum of four Lorentzian sextets. Relative areas of the lines in each sextet were constrained in the ratios 3:2:1:1:2:3 as is required for a randomly oriented powder sample. Different linewidths were fixed for the inner, middle and outer pairs of lines. The relative intensity ratios for each of the spectral components were constrained to nearly 6:9:18:18 corresponding to the site occupancy of Fe atoms in the crystal structure. To obtain an acceptable fit, we compared the values of χ^2 for the different possible fits to the same spectra.

The best fits are shown by the full curves in figure 2. The examples of the subspectra corresponding to various sites for $\text{Er}_2\text{Fe}_{17}\text{C}_{2.5}$ at 12 and 70 K are plotted as broken curves in figure 2. The results indicate that the order of the effective hyperfine field values is $6c > 18f, 18h > 9d$. The hyperfine splitting of the dumbbell sites (6c site) is larger than those of the other three. This is consistent with the early results given by most workers

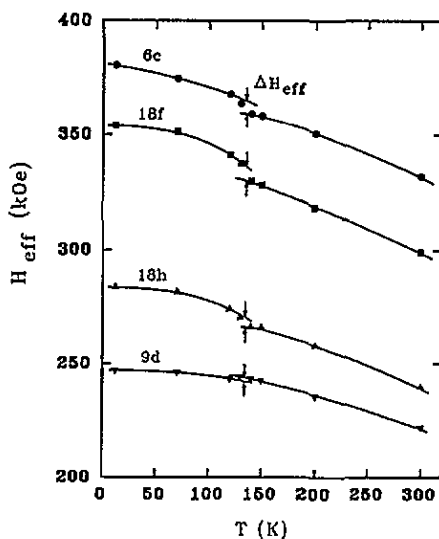


Figure 3. Temperature dependence of the effective hyperfine fields of the four iron sites for $\text{Er}_2\text{Fe}_{17}\text{C}_{2.5}$. The full curves are guides to the eye.

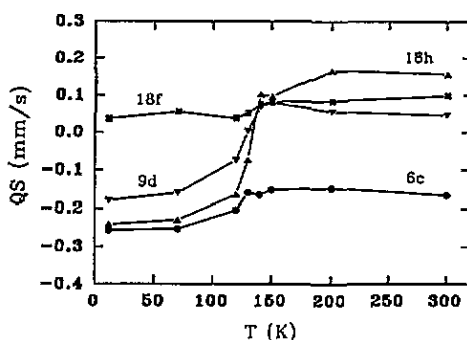


Figure 4. Temperature dependences of the Qs of the four iron sites for $\text{Er}_2\text{Fe}_{17}\text{C}_{2.5}$.

[3–5]. The assignment of the 9d sites is similar to that of 6g in $\text{Er}_2\text{Fe}_{17}\text{C}$ obtained by Gubbens *et al* [13]. To distinguish between the two subspectra with the same number of site occupancies, we have to consider the nearest-neighbour environments. Many workers assign the larger hyperfine fields to the sites with a larger number of iron neighbours and a smaller number of rare-earth neighbours. The 18f sites have ten iron and two rare-earth neighbours, whereas the 18h sites have nine iron and three rare-earth neighbours. This suggests that the Fe atoms of 18f sites have a larger hyperfine field than those of 18h sites.

For the spectra above T_{ST} , the order of the hyperfine fields is also taken to be $6c > 18f > 18h > 9d$. A further subdivision of 18f, 18h and 9d sites into two groups with relative intensity ratio 1:2 is assumed. Therefore the spectra are analysed with seven independent Lorentzian sextets. The best fits are also shown by the full curves in figure 2.

The effective hyperfine fields H_{eff} , the quadrupole splittings (Qs) and the isomer shifts (ISs) of the four iron sites are summarized in tables 1–3. The hyperfine parameters of 18f, 18h and 9d sites are derived from the corresponding two subspectra by weighting the values

with 1:2. The average hyperfine fields (H_{eff}) are obtained by weighting the contribution of the various sites. The ISS are given relative to $\alpha\text{-Fe}$ at room temperature.

Table 1. The fitted effective hyperfine fields H_{eff} and average hyperfine fields ($\langle H_{\text{eff}} \rangle$) deduced from ^{57}Fe Mössbauer spectra of $\text{Er}_2\text{Fe}_{17}\text{C}_{2.5}$ at various temperatures. ΔH_{eff} , the change in H_{eff} at around T_{sr} , is also shown.

T (K)	H_{eff} (kOe)				$\langle H_{\text{eff}} \rangle$ (kOe)	χ^2
	6c	18f	18h	9d		
12	380	354	284	247	314	1.88
70	375	351	282	246	311	2.03
120	368	341	275	243	303	1.81
130	364	337	271	244	301	2.02
140	359	329	267	243	296	1.63
150	358	328	267	242	295	1.61
200	351	318	259	235	286	1.54
300	331	299	240	222	268	1.72
ΔH_{eff} (kOe)	7	7	5	-1		

Figure 3 plots the temperature dependence of the hyperfine fields and the full curves serve to guide the eye. A discontinuity appears at around T_{sr} where the spin reorientation transition takes place. In fact, the transition of the easy-magnetization direction has a large temperature region. As seen from figure 3, the decrease in the hyperfine fields for 6c, 18f and 18h sites become more rapid at about 120 K, and the strongest decrease occurs at T_{sr} . By extrapolating the H_{eff} versus T curve below T_{sr} and that above T_{sr} we can estimate ΔH_{eff} (the change in H_{eff}) at around T_{sr} . These values are also listed in table 1.

The temperature dependences of QS and IS are plotted in figure 4 and in figure 5, respectively. A leap is observed in the QS versus T curves at around T_{sr} with increasing temperature. The change in QS is evident from figure 2. Compared with the spectra below 136 K, lines 2 shift away from lines 1 and lines 5 shift to lines 6 for spectra above 136 K. The QS-values are determined by the above four positions. The ISS also show an anomaly for the 6c sites at around T_{sr} .

4. Discussion

The discontinuity at about 136 K in figure 3 shows a hyperfine field anisotropy in $\text{Er}_2\text{Fe}_{17}\text{C}_{2.5}$. It is known that the effective hyperfine field consists of isotropic and anisotropic parts. The latter mainly results from the orbital moment contribution and the dipolar contribution which are easily calculated. Deportes *et al* [14] find that the dipolar contribution is much smaller than the orbital contribution in Y_2Fe_{17} , and that the anomaly in the hyperfine field variation is attributed to the increase in the orbital contribution when the Fe magnetic moments rotate from their easy-magnetization direction to their hard-magnetization direction. Since the local symmetries of each Fe site are different, the change in the hyperfine field at around 136 K differs for various sites.

The hyperfine field anisotropy can be used to estimate roughly the anisotropy of the iron atomic magnetization. The ΔH_{eff} -value of the 6c-site atoms for $\text{Er}_2\text{Fe}_{17}\text{C}_{2.5}$ is about 7 kOe, smaller than that (about 26 kOe) of dumbbell sites observed in Y_2Fe_{17} [14]. This

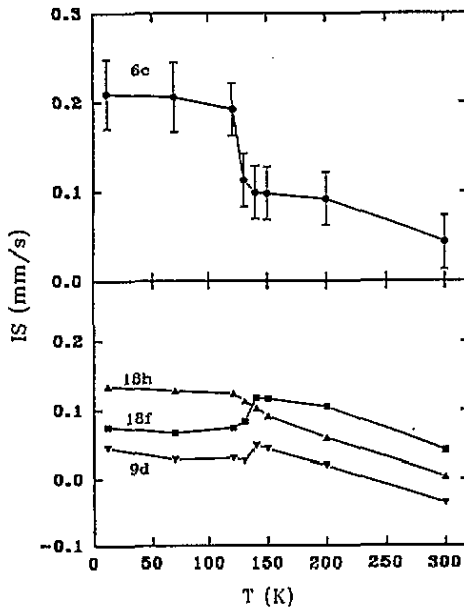


Figure 5. Temperature dependences of the ISS of the four iron sites for $\text{Er}_2\text{Fe}_{17}\text{C}_{2.5}$.

reflects that the interstitial C atoms may lead to a decrease in the magnetic anisotropy of the iron atoms.

As is seen from figure 3, the hyperfine field of 9d sites has an opposite change to those of 6c, 18f and 18h sites. This suggests that the magnetic anisotropy of 9d sites is probably different from the planar anisotropy of the three other sites.

The QSs exhibit an increase at T_{sr} with increasing temperature, and the increases are different for different sites. In the ^{57}Fe Mössbauer effects of most rare-earth-iron compounds, the quadrupole interaction is sufficiently small to be treated as a perturbation. Therefore the QS can be given by [15]

$$QS = -\frac{1}{4}e^2qQ'[1 - 3\cos^2\Theta - \eta\sin^2\Theta\cos(2\Phi)] \quad (1)$$

where (Θ, Φ) defines the direction of the hyperfine field in the framework of the EFG, $eq = V_{zz'}$ is the principal component of the EFG with direction z' , and Q' is the quadrupole moment of the excited state of the ^{57}Fe nucleus. When the iron moment direction turns from parallel to the c axis to perpendicular to the c axis, the pole angle Θ changes. This explains why the QS shows an anomaly at T_{sr} . It is noted that the splittings for the 9d and 18f sites change sign on spin reorientation while those for the 6c and 18h sites do not. The different changes may be due to the different η -values of the last term in equation (1), for η is related to the surroundings of the iron sites. The behaviour of QS around T_{sr} indicates that QS in $\text{R}_2\text{Fe}_{17}\text{C}_x$ is sensitive to the easy-magnetization direction. A similar tendency was observed in early studies of $\text{R}_2\text{Fe}_{14}\text{B}$ [15]. It has been found that the QS-value at the $8j_1$ sites for $\text{R}_2\text{Fe}_{14}\text{B}$ with the easy-magnetization direction perpendicular to the c axis has an opposite sign to the rest of the series for which the easy-magnetization direction is parallel to the c axis.

Another trend is that the ISS for the 6c sites show a decrease (see figure 5). The decrease can be found directly from the experimental spectra. The 6c sites have the largest hyperfine

Table 2. The fitted QSS deduced from ^{57}Fe Mössbauer spectra of $\text{Er}_2\text{Fe}_{17}\text{C}_{2.5}$ at various temperatures.

T (K)	QS (mm s^{-1})			
	6c	18f	18h	9d
12	-0.26	0.04	-0.24	-0.18
70	-0.25	0.06	-0.23	-0.16
120	-0.20	0.04	-0.16	-0.07
130	-0.16	0.05	-0.07	0.00
140	-0.16	0.08	0.10	0.07
150	-0.15	0.08	0.10	0.08
200	-0.15	0.08	0.17	0.06
300	-0.16	0.10	0.16	0.05

Table 3. The fitted ISS (relative to $\alpha\text{-Fe}$ at room temperature) deduced from the ^{57}Fe Mössbauer spectra of $\text{Er}_2\text{Fe}_{17}\text{C}_{2.5}$ at various temperatures.

T (K)	IS (mm s^{-1})			
	6c	18f	18h	9d
12	0.21	0.07	0.13	0.04
70	0.21	0.07	0.13	0.03
120	0.19	0.07	0.12	0.03
130	0.11	0.08	0.11	0.03
140	0.10	0.12	0.10	0.05
150	0.10	0.12	0.09	0.04
200	0.09	0.10	0.06	0.02
300	0.04	0.04	0.00	-0.04

splitting corresponding to the outermost lines. As is seen in figure 2, the outermost smaller peaks of the spectra above T_{sr} slightly shift to the left, which indicates that the IS decreases. The same result was observed in $\text{Er}_2\text{Fe}_{17}\text{C}_x$ with lower C contents [16]. We have no explanation for this at present.

Acknowledgments

This work was supported by the National Natural Science Foundation of China and the award of a Post-Doctoral Fellowship.

References

- [1] Buschow K J H 1991 *Rep. Prog. Phys.* **54** 1123
- [2] Steiner W and Haferl R 1977 *Phys. Status Solidi* **a** **42** 739
- [3] Zouganelis G, Anagnostou M and Niarchos D 1991 *Solid State Commun.* **77** 11
- [4] Gubbens P C M, van Apeldoorn J H F, van der Kraan A M and Buschow K H J 1974 *J. Phys. F: Met. Phys.* **4** 921
- [5] Hu B P, Li H S, Sun H and Coey J M D 1991 *J. Phys.: Condens. Matter* **3** 3983
- [6] Coey J M D and Sun H 1990 *J. Magn. Magn. Mater.* **87** L251
- [7] Katter K, Wecker J, Schultz L and Grossinger R 1990 *J. Magn. Magn. Mater.* **92** L14
- [8] Coey J M D, Sun H, Otani Y and Hurley D P F 1991 *J. Magn. Magn. Mater.* **98** 76

- [9] Shen Bao-gen, Kong Lin-shu and Cao Lei 1992 *Solid State Commun.* **83** 753
- [10] Cao Lei, Kong Lin-shu and Shen Bao-gen 1992 *J. Phys.: Condens. Matter* **4** L515
- [11] Hu Bo-ping and Liu Gui-chuan 1991 *Solid State Commun.* **79** 785
- [12] Qi Qi-nian, San Hong and Coey J M D 1992 *J. Alloys Compounds* **182** 313
- [13] Gubbens P C M, van der Kraan A M, Jacobs T H and Buschow K H J 1990 *J. Less-common Met.* **163** 165
- [14] Deportes J, Kebe B and Lemaire R 1986 *J. Magn. Magn. Mater.* **54** 1089
- [15] Fruchart R, Heritier P L, Dalmas de Reotier P, Fruchart D, Wolfers P, Coey J M D, Ferrierra L P, Guillen R, Vulliet P and Yaounc A 1987 *J. Phys. F: Met. Phys.* **17** 483
- [16] Kong Lin-shu, Shen Bao-gen, Cao Lei, Gong Hua-yang and Chen Yi-long 1993 *Solid State Commun.* at press